Chinese Chemical Letters 28 (2017) 839–844

Contents lists available at ScienceDirect

Chinese Chemical Letters

journal homepage: www.elsevier.com/locate/cclet

Original article

Fabrication of virus-like particles with strip-pattern surface: A two-step self-assembly approach

Shuo Zhang, Chun-Hua Cai*, Zhou Guan, Jia-Ping Lin*, Xing-Yu Zhu

Shanghai Key Laboratory of Advanced Polymeric Materials, State Key Laboratory of Bioreactor Engineering, Key Laboratory for Ultrafine Materials of Ministry of Education, School of Materials Science and Engineering, East China University of Science and Technology, Shanghai 200237, China

ARTICLE INFO

Article history:
Received 5 September 2016
Received in revised form 18 October 2016
Accepted 24 October 2016
Available online 8 January 2017

Keywords:
Virus-like particles
Two-step self-assembly
Striped patterns
Defects
Polypeptide
Ordered structure

ABSTRACT

Spherical nanostructures with striped patterns on the surfaces resembling the essential structures of natural virus particles were constructed through a two-step self-assembly approach of polystyrene-*b*-oligo(acrylic acid) (PS-*b*-oligo-AA) and poly(γ-benzyl L-glutamate)-*b*-poly(ethylene glycol) (PBLG-*b*-PEG) copolymer mixtures in solution. On the basis of difference in hydrophilicity and self-assembly properties of the two copolymers, the two-step self-assembly process is realized. It was found that PS-*b*-oligo-AA copolymers formed spherical aggregates by adding a certain amount of water into polymer solutions in the first step. In the second step, two polymer solutions were mixed and water was further added, inducing the self-assembly of PBLG-*b*-PEG on the surfaces of PS-*b*-oligo-AA spheres to form striped patterns. In-depth study was conducted for the indispensable defects of striped patterns which are dislocations and +1/2 disclinations. The influencing factors such as the mixing ratio of two copolymers and the added water content in the first step on the morphology and defects of the striped patterns were investigated. This work not only presents an idea to interpret mechanism of the cooperative self-assembly behavior, but also provides an effective approach to construct virus-like particles and other complex structures with controllable morphology.

1. Introduction

Amphiphilic copolymers are able to self-assemble into various supramolecular aggregates [1–8]. Inspired by biological systems in nature, researchers have regarded the fabrication of hierarchical nanostructures that resemble natural materials as one of the topics of macromolecular self-assembly in recent years [9–13]. For example, virus is an ideal model for polymer self-assembly which possesses well-defined architectures with a protein capsid and encapsulated genetic materials as the core [14]. Virus-like particles (VLPs) are promising for biomedical potential in drug/gene delivery and functional imaging [12,15–17]. Amphiphilic polypeptides gained special attentions for the fabrication of VLPs, as they are analogous with natural protein in chemical component [13,18–25]. Furthermore, polypeptide-based VLPs could be more stable and feasible in functionalization due to the high molecular weight and abundant modifiable groups of polypeptides [26–31].

Due to the precise core-shell structure of the virus, the fabrication of VLPs is a challenging work. In our previous works, polypeptide-based spherical VLPs were obtained by the self-assembly of poly(γ-benzyl L-glutamate)-*b*-poly(ethylene glycol) (PBLG-*b*-PEG) rod-coil block copolymer and polystyrene (PS) homopolymer mixtures [22,23]. It was found that PS homopolymers aggregated into spheres and PBLG-*b*-PEG block copolymers formed striped patterns on the surfaces of the PS spheres. However, since the primarily formed hydrophobic PS spheres are not stable in solution, the specific formation process and the details of the complex structures cannot be confirmed. As indicated by literatures, for the construction of complex nanostructures, multi-step self-assembly processes have been proven to be rather elegant and feasible. This method not only provides a versatile approach to design complex nanostructure in a controllable way, but also gives a clear pathway for the aggregation process [32–38].

Herein, a two-step solution self-assembly method was applied to achieve controllable fabrication of spherical VLPs from polystyrene-*b*-oligo-(acrylic acid) (PS-*b*-oligo-AA) copolymers and PBLG-*b*-PEG copolymers. Copolymers were dissolved in THF/DMF mixture solvent separately, and a self-assembly was

* Corresponding authors.
E-mail addresses: caichunhua@ecust.edu.cn (C.-H. Cai), jlin@ecust.edu.cn (J.-P. Lin).

http://dx.doi.org/10.1016/j.cclet.2016.12.040

driven by adding water. In the first step, with adding water PS-*b*-oligo-AA self-assembled into spherical aggregates (PS spheres covered with oligo-AA shell). In the second step, further assembly of PBLG-*b*-PEG on the surfaces of PS-*b*-oligo-AA spheres into strips was induced by mixing the two polymer solutions and subsequent addition of water. The morphologies and structures of the final aggregates were found to be controlled by the mixing ratio of the two polymers and the added water content in the first step.

2. Results and discussion

The two-step self-assembly process fabricating the virus-like particles with strip-pattern surface is illustrated as follows. PS-*b*-oligo-AA copolymers and PBLG-*b*-PEG copolymers were initially dissolved separately with THF/DMF mixture solvent (1/1, v/v). In the first step, with a certain amount of water added to the solutions, PS-*b*-oligo-AA copolymers were able to self-assemble into spheres with oligo-AA chains outspreading and providing colloidal stability for the aggregates, while PBLG-*b*-PEG copolymers packed loosely forming irregular aggregates. In the second step, the two solutions were mixed together, and more water was added, which induced the self-assembly of PBLG-*b*-PEG block copolymers on the surfaces of PS-*b*-oligo-AA spheres. The structure of the VLPs and the influencing factors on the structure of the formed VLPs are studied.

2.1. Structure of VLPs self-assembled through a two-step self-assembly process

We first investigated the self-assembly behaviors of the two single copolymers, respectively. Fig. 1a shows the turbidity of the copolymer solutions against water content. At lower water content, the absorbance values of the two copolymer solutions are close to zero and negligible changes in the magnitude of absorption are observed. As water content reaches a certain value, the turbidity intensity increases dramatically, corresponding to the onset of aggregation of the copolymers. The amount of the added water at which aggregates start to form is defined as the critical water content (CWC) and obtained from the sudden change in the absorbance value during turbidity testing (the water addition process) [21,42–45]. As can be seen, the CWC values of the PS-*b*-oligo-AA and PBLG-*b*-PEG copolymer solutions are about 8.6 wt% and 14.4 wt%, respectively, which indicates that PS-*b*-oligo-AA copolymer is more hydrophobic than PBLG-*b*-PEG copolymer.

In addition, as revealed by the turbidity curves, the absorbance value of PS-*b*-oligo-AA copolymer solution increases sharply with water content and reaches a plateau after the water content exceeds 16 wt%. TEM image shows that PS-*b*-oligo-AA copolymers

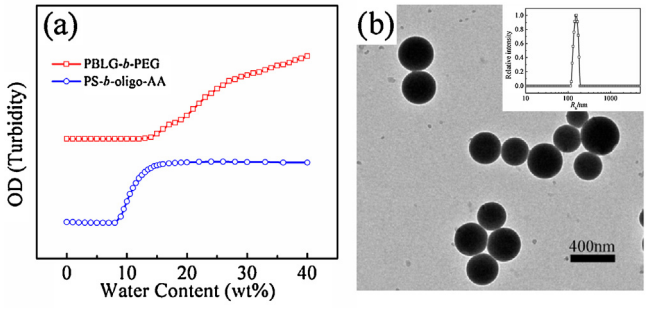

Fig. 1. (a) Turbidity (optical density) curves of PBLG-*b*-PEG and PS-*b*-oligo-AA solutions in THF/DMF = 1/1 in volume at the initial concentration of 0.2 gL^{-1} as a function of the amount of water added to the solution. (b) Typical TEM image of PS-*b*-oligo-AA at water content of 16 wt%. Inset plot is hydrodynamic radius distribution of aggregates in solution (scattering angle is 90°).

formed spherical aggregates (PS-*b*-oligo-AA spheres) with diameter ranging from 250 nm to 350 nm at the water content of 16 wt% (Fig. 1b). In the following content, we use "PS spheres" to refer the PS-*b*-oligo-AA spheres as the AA chains hardly have any effect. The size of the PS spheres is further characterized by DLS testing. As shown in the inset of Fig. 1b, the PS spheres possess a mean hydrodynamic radius (<R_h>) of 143 nm with a narrow size distribution, and the polydispersity index (PDI) is around 0.04. The DLS result is in good consist with TEM observation. After the water content exceeds 16 wt%, no obvious change of the morphology and size of the PS spheres was observed (see Supporting information, Fig. S2a and 2b), suggesting that the structure of the PS-*b*-oligo-AA copolymer aggregates remains unchanged and stable in a wide range of water content.

For PBLG-*b*-PEG copolymers, as shown in Fig. 1a, the absorbance value keeps increasing with the water content in a relative wide range above the CWC value. This indicates that PBLG-*b*-PEG copolymers cannot form stable aggregates in such a wide range of water content. As revealed by TEM testing (picture is not shown), no aggregate is observed at the water content of 16 wt% (close to CWC value). While at a higher water content of 32 wt%, irregular structures are observed, which indicates that PBLG-*b*-PEG copolymers do not form stable aggregates and the copolymer chains have high mobility (for details, see Supporting information, Fig. S2c).

The above experiments revealed that, PS-*b*-oligo-AA copolymers formed stable PS spheres in a wide range of added water content in the first step (for example, 16–32 wt%), while PBLG-*b*-PEG copolymers still had high mobility. It can be deduced that after mixing these two copolymer solutions prepared in the first step and further adding water in the second step, PBLG-*b*-PEG copolymers can self-assemble on the surfaces of PS spheres. SEM observations of the aggregates obtained through the two-step self-assembly confirmed our predictions. The results are shown in Fig. 2 and Fig. S3. It was found that when the weight fraction of PBLG-*b*-PEG in the mixture was low, for example, $f_{PBLG\text{-}b\text{-}PEG} = 0.1$, spheres with smooth surfaces were formed (Fig. 2a). Increasing the weight fraction of PBLG-*b*-PEG in the mixture, spherical aggregates with ordered striped patterns on the surfaces (strip-pattern spheres, like "wool-balls") were obtained. The patterns are formed by the ordered packing of rigid PBLG blocks, and hydrophilic PEG chains stabilize the aggregates. Details for the structure of the striped patterns can be found in our previous works [22,23]. Shown in Fig. 2b–d are the SEM images of the strip-pattern spheres formed with $f_{PBLG\text{-}b\text{-}PEG} = 0.3$, 0.5, and 0.7, respectively. As can be seen, the thickness of the shell and the width of the strips increase with the weight fraction of PBLG-*b*-PEG in the mixtures. Especially in Fig. 2d, the strips formed by the further self-assembly of PBLG-*b*-PEG block copolymers are found to be much thicker. This phenomenon caused that the VLPs look special and the cores (PS spheres with oligo-AA shell) look small. Shown in Fig. 2e is a typical TEM image of the aggregates formed with $f_{PBLG\text{-}b\text{-}PEG} = 0.5$, which confirms the formation of strip-pattern spheres. When the weight fraction of PBLG-*b*-PEG in the mixtures is higher ($f_{PBLG\text{-}b\text{-}PEG} \geq 0.7$), the strips become very thick and the morphology of the aggregates becomes irregular. Meanwhile, some small aggregates which should be formed by PBLG-*b*-PEG copolymers were observed (Fig. S3a in Supporting information).

The size of the aggregates was further characterized by DLS testing. For the aggregates formed with $f_{PBLG\text{-}b\text{-}PEG}$ in the range of 0.1–0.5, the size distribution shows a narrow single peak, indicating the aggregates are uniform in size. Shown in the inset plot of Fig. 2e is a typical DLS result for the aggregates formed with $f_{PBLG\text{-}b\text{-}PEG} = 0.5$ which gives a mean hydrodynamic radius of 168 nm and a PDI value of 0.05. When $f_{PBLG\text{-}b\text{-}PEG}$ is higher than 0.7, a broader peak is observed in DLS result (Fig. S3b in Supporting information), which is in correspondence with the fact that the

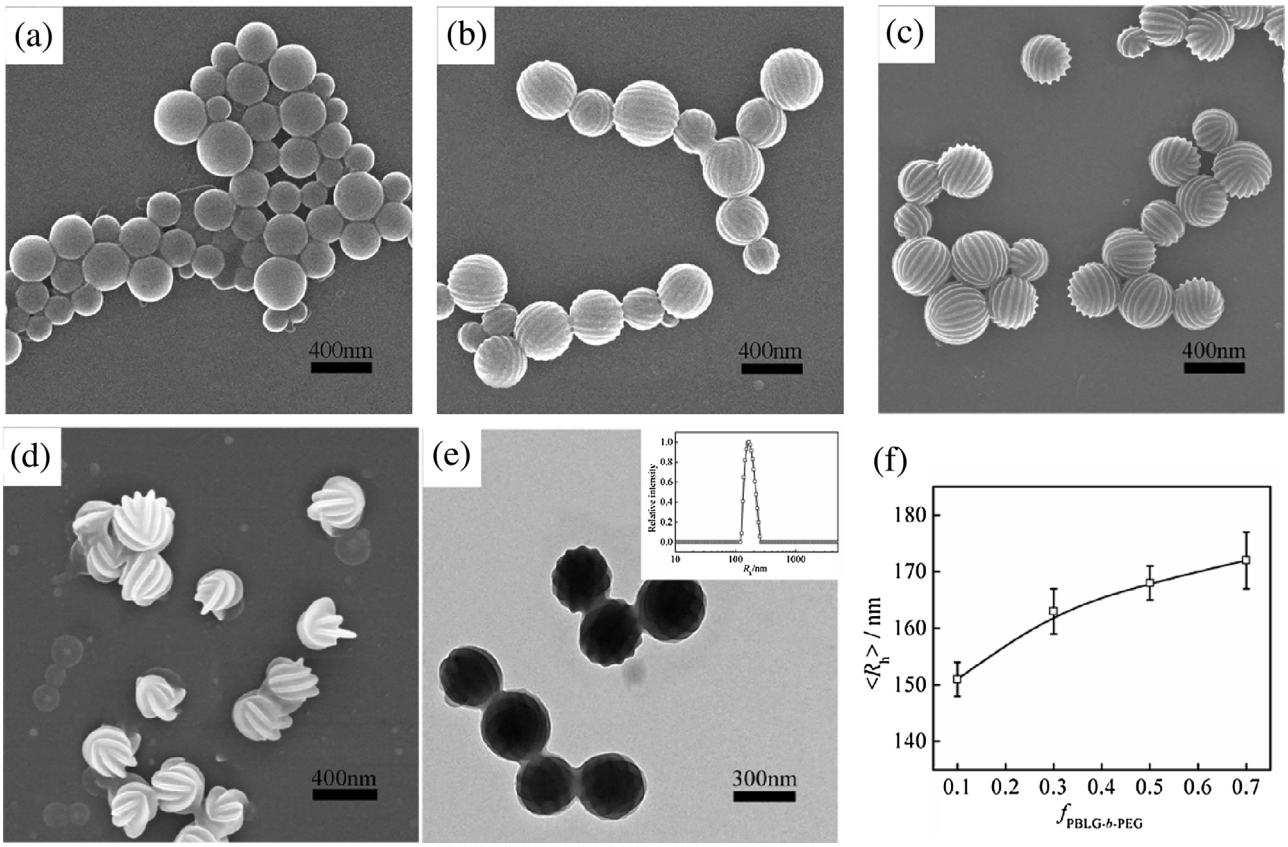

Fig. 2. Typical SEM images of aggregates self-assembled through a two-step process with various $f_{PBLG\text{-}b\text{-}PEG}$: (a) $f_{PBLG\text{-}b\text{-}PEG}$ = 0.1, (b) $f_{PBLG\text{-}b\text{-}PEG}$ = 0.3, (c) $f_{PBLG\text{-}b\text{-}PEG}$ = 0.5, and (d) $f_{PBLG\text{-}b\text{-}PEG}$ = 0.7. (e) Typical TEM image of aggregates self-assembled through a two-step process with $f_{PBLG\text{-}b\text{-}PEG}$ = 0.5. Inset plot of (e) is hydrodynamic radius distribution of aggregates in water (scattering angle is 90°). (f) Plot of $<R_h>$ versus the $f_{PBLG\text{-}b\text{-}PEG}$. The added water content in the first step is 16 wt%.

solution contains additional small aggregates formed by PBLG-*b*-PEG copolymers themselves. The size variation of the aggregates as a function of $f_{PBLG\text{-}b\text{-}PEG}$ is plotted in Fig. 2f. As can be seen, the radius of the aggregates gradually increases from 151 nm ($f_{PBLG\text{-}b\text{-}PEG}$ = 0.1) to 173 nm ($f_{PBLG\text{-}b\text{-}PEG}$ = 0.7). These DLS results are in good agreement with SEM and TEM observations.

For the strip-pattern spheres, there exist defects, *i.e.* dislocations, +1/2 disclinations, and −1/2 disclinations, which is an important natural geometrical phenomenon [46–50]. In the present system, −1/2 disclination defect was rarely observed, while dislocation and +1/2 disclination defects were identified. SEM images of the dislocation and +1/2 disclination defects are presented in Fig. 3a and b, respectively. The insets display schematic illustrations of the defects. In addition, for the striped patterns on spheres, the total disclination charges is a constant value (+2) [23,50]. Therefore, each strip-pattern sphere should contain four +1/2 disclination defects. Hence, the dislocation number variation of these strip-pattern spheres is investigated in the following context.

The dependence of the dislocation number on mixing ratio was plotted in Fig. 3c. The dislocation number was counted based on large number of SEM images. It should be noted that, SEM images only reflect approximately 3/8 of the total area of the spherical surface for each ball, therefore, only the defect number in this observed area can be counted. And the total number of defects is calculated based on the reasonable assumption that the defects on sphere surface are randomly distributed. As can be seen, with increasing $f_{PBLG\text{-}b\text{-}PEG}$, the total number of dislocation defects decreases first and then becomes constant. The main reason could be the decrease of the number of strips on the surfaces of PS

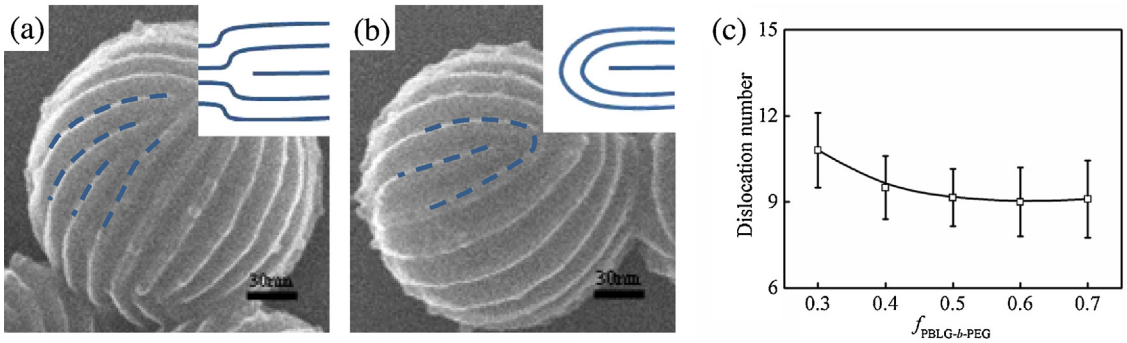

Fig. 3. SEM images of classical defects configuration: (a) dislocations and (b) +1/2 disclination. Inset plots are schematic illustration. (c) Statistic dislocation number as a function of $f_{PBLG\text{-}b\text{-}PEG}$. The added water content in the first step is 16 wt% with $f_{PBLG\text{-}b\text{-}PEG}$ = 0.5.

spheres with increasing $f_{PBLG\text{-}b\text{-}PEG}$. As shown in Fig. 2b–d, when $f_{PBLG\text{-}b\text{-}PEG} < 0.5$, the width of the strips increases and the number of strips on each sphere decreases markedly with increasing $f_{PBLG\text{-}b\text{-}PEG}$. Considering the average size of the core PS spheres does not change with $f_{PBLG\text{-}b\text{-}PEG}$ in the mixtures, the dislocation number on each sphere decreases about from eleven to nine. while at high $f_{PBLG\text{-}b\text{-}PEG}$ (for example, $f_{PBLG\text{-}b\text{-}PEG} \geq 0.5$), both the width of the strips and the number of strips on each sphere almost keep constant with $f_{PBLG\text{-}b\text{-}PEG}$. The number of dislocations is unchanged, which maintains around nine.

2.2. Effect of the added water content in the first step on the structure of VLPs

As mentioned above, PBLG-*b*-PEG copolymers form unstable aggregates and possess a high mobility in a relative wide range of water content. Therefore, it can be deduced that VLPs would be obtained in a wide range of added water content in the first step. As shown in Fig. 4, it was found that when the added water content in the first step increases from 16 wt% to 20 wt% and 24 wt%, the striped patterns on spheres become thinner (Fig. 4a and b). The strips almost disappear when the added water content in the first step increases to 32 wt% (Fig. 4c). Meanwhile, more small aggregates formed by pure PBLG-*b*-PEG were observed with increasing the added water content in the first step. These results indicate that the mobility of PBLG-*b*-PEG copolymer chains is dramatically weakened when the added water content in the first step is higher. With further adding water in the second step, few PBLG-*b*-PEG copolymers can be adsorbed onto the PS spheres. As a result, the striped patterns become thinner and more irregular and the number of dislocations increases obviously with added water content in the first step (Fig. 4d).

Based on the investigations, the mechanism of the two-step self-assembly process fabricating the spherical virus-like particles with strip-pattern surface is illustrated (Scheme 1). Initially, PS-*b*-oligo-AA copolymers and PBLG-*b*-PEG copolymers were dissolved with THF/DMF mixture solvent (1/1, v/v) respectively. In the first step, with certain amount of water added into the two copolymer solutions in THF/DMF mixture solvent (1/1 in volume), PS-*b*-oligo-AA copolymers self-assembled into spherical aggregates, while PBLG-*b*-PEG copolymers packed loosely and formed unstable and irregular aggregates. In the second step, the two solutions were mixed together. Upon further addition of water, the PBLG-*b*-PEG copolymers self-assembled on the surfaces of PS spheres and packed orderly to form striped patterns. From the formation mechanism (Scheme 1) we can see the distinguished structural feature of the aggregates and the clear core-shell structure which mimics the essential structure of natural virus. 1) PS-*b*-oligo-AA copolymers form spheres and serve as template mimicking the role of nucleic acid in virus core; 2) PBLG-*b*-PEG copolymers cover the PS-*b*-oligo-AA spheres and pack orderly into specific patterns mimicking the role of the capsid protein.

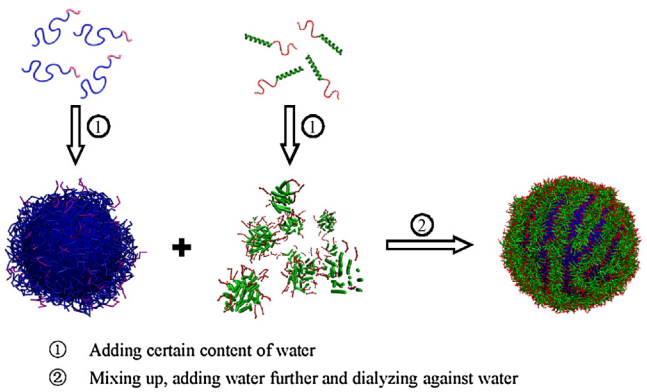

Scheme 1. Schematic representation for the fabrication of spherical virus-like particles with strip-pattern surface through a two-step self-assembly process.

The two-step self-assembly process is believed to provide attractive advantages in achieving controllable hierarchical structures. Interpretation of some cooperative self-assembly mechanism and intense research on supramolecular chemistry can also be achieved by the approach. The investigation of virus-like particles with hierarchical nanostructures resembling natural biological structures such as poxviridae can promote better understanding of the biological patterns in nature.

3. Conclusion

In summary, spherical virus-like particles with strip-pattern surface were prepared through a two-step self-assembly process. In the first step, small amount of water was added into PS-*b*-oligo-AA and PBLG-*b*-PEG solutions (in THF/DMF mixture) separately, which induced the self-assembly of PS-*b*-oligo-AA copolymers into spherical aggregates (PS spheres with oligo-AA shell). While PBLG-*b*-PEG copolymers formed irregular and unstable aggregates due to different hydrophobicity of the two copolymers. In the second step, two copolymer solutions were mixed up and more water was added, which drives the further self-assembly of PBLG-*b*-PEG on the PS-*b*-oligo-PAA spheres to form striped patterns. The strip-pattern spheres possess the defects of dislocations and +1/2 disclinations. The number of +1/2 disclinations is fixed at four for each strip-pattern spheres, while the number of dislocations decreases with decreasing the added water content in the first step.

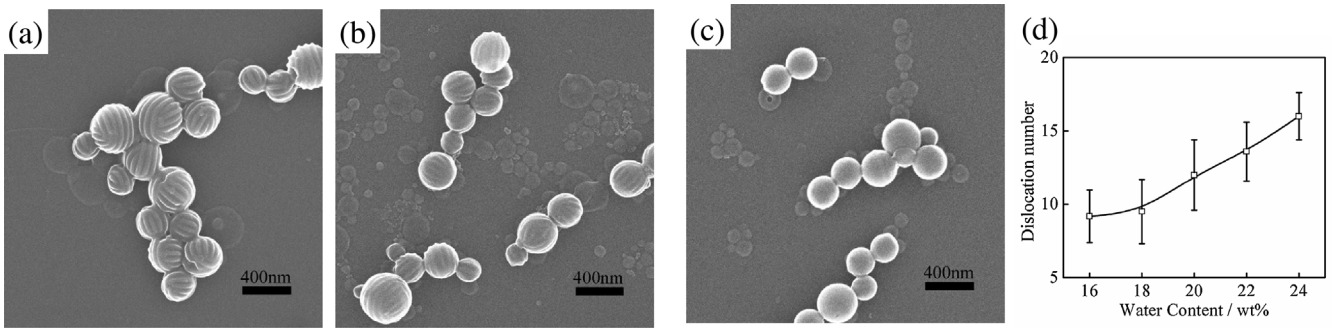

Fig. 4. (a-c) Typical SEM images of aggregates self-assembled through a two-step process with various added water contents in the first step: (a) 20 wt%; (b) 24 wt% and (c) 32 wt%. (d) Statistic dislocation number as a function of added water content in the first step. $f_{PBLG\text{-}b\text{-}PEG} = 0.5$.

4. Experimental

Materials and regents: PS_{102}-*b*-oligo-AA_8 copolymers and $PBLG_{55}$-*b*-PEG_{112} copolymers (the subscripts denote the degree of polymerization for each segment) were synthesized according to the literatures [39–41]. The details for the synthesis and characterization of the polymers are presented in the Supporting Information Section 1. Tetrahydrofuran (THF), *N,N'*-dimethylformamide (DMF), and all the other regents were of analytical grade and used as received (purchased from Adamas-beta). Deionized water was prepared in a Millipore Super-Q Plus Water System to a level of 18.2 MΩ cm resistance. Dialysis bag (Membra-cel, 3500 molecular weight cutoff) was provided by Serva Electrophoresis GmbH.

Turbidity testing of the polymer solutions: The optical density (turbidity) was measured at a wavelength of 690 nm (which was far from the absorption of the benzene chromophore) using a quartz cell (path length: 1 cm) with a UV–vis spectrophotometer (UV-vis UV-2550 Shimadzu). Both the PS-*b*-oligo-AA and the PBLG-*b*-PEG copolymers were first dissolved in THF/DMF mixture solvent (1/1, v/v) separately with a concentration of 0.2 g/L. Deionized water was then added drop by drop (0.02 mL per drop to 2 mL of polymer solution) with vigorous stirring. And after each drop of deionized water was added, the solution was stirred for 1 min and then left to equilibrate for 2 min or more until the optical density was stable.

Preparation of aggregates through a two-step self-assembly process: The polymeric self-assemblies were prepared using a selective solvent method through a two-step process. In the first step, PS-*b*-oligo-AA and PBLG-*b*-PEG block copolymers were separately dissolved in THF/DMF mixture solvent (1/1, v/v) by stirring at room temperature for 2 days to obtain stock solutions. Then, a certain amount of deionized water (typically 0.32 mL, 16 wt %), a selective solvent for oligo-AA and PEG, was added into the two solutions (2 mL) respectively at a rate of 0.5 mL/min with vigorous stirring. The weight percent of the added water is defined as the ratio of water weight to the original weight of organic solutions. In this situation, PS-*b*-oligo-AA copolymers self-assemble into spherical aggregates (PS spheres covered with oligo-AA shell), while PBLG-*b*-PEG copolymers pack loosely forming irregular morphology. In the second step, the two solutions were mixed up with various volume ratios and stabilized with stirring (4 hours). Typically, the weight fraction of PBLG-*b*-PEG, $f_{\mathrm{PBLG\text{-}b\text{-}PEG}}$, which is defined as the ratio of weight of PBLG-*b*-PEG to the total weight of mixture copolymers, was in the range of 0.1–0.7. Then more deionized water was added to the mixed solution. Finally, by dialysis against deionized water for 3 days to remove all the organic solvents, spherical virus-like core-shell aggregates were obtained. Before analysis, the solutions were stabilized for at least 5 days.

Testing apparatus and method: The morphologies of aggregates were examined by TEM (JEM-1400, JEOL) operated at an accelerating voltage of 100 kV. The TEM samples were prepared by placing drops of solution on a copper grid coated with carbon film and then dried at room temperature. The morphologies of aggregates were also observed by SEM (S4800, Hitachi) operated at an accelerating voltage of 15 kV. The samples were prepared the same as TEM samples. Before the observations, the samples were sputtered by Aurum. Dynamic laser scattering (DLS) was measured by a LLS spectrometer (ALV/CGS-5022F) equipped with an ALV-High QE APD detector and an ALV-5000 digital correlator using a He-Ne laser (the wavelength $\lambda = 632.8$ nm) as the light source. All the samples were filtered through 0.8 μm filters to remove dust before DLS measurements, and all the measurements were carried out at 25 °C.

Acknowledgments

This work was supported by the National Natural Science Foundation of China (Nos. 21234002, 51303055, 21474029, and 51573049). Support from projects of Shanghai municipality (Nos. 15QA1401400 and 13JC1402000) is also appreciated.

Appendix A. Supplementary data

Supplementary data associated with this article can be found, in the online version, at http://dx.doi.org/10.1016/j.cclet.2016.12.040.

References

[1] Y.Y. Mai, A. Eisenberg, Self-assembly of block copolymers, Chem. Soc. Rev. 41 (2012) 5969–5985.
[2] D.E. Discher, A. Eisenberg, Polymer vesicles, Science 297 (2002) 967–973.
[3] A.H. Gröschel, A. Walther, T.I. Löbling, et al., Guided hierarchical co-assembly of soft patchy nanoparticles, Nature 503 (2013) 247–251.
[4] L.L. Chen, T. Jiang, J.P. Lin, C.H. Cai, Toroid formation through self-assembly of graft copolymer and homopolymer mixtures: experimental studies and dissipative particle dynamics simulations, Langmuir 29 (2013) 8417–8426.
[5] F.B. Zhao, Z.L. Liu, J.P. Sun, L. Feng, J.W. Hu, Optically active micelles from self-assembly of MPEG-*b*-PMALM copolymer in water, Chin. Chem. Lett. 20 (2009) 231–234.
[6] D.Y. Yan, Y.F. Zhou, J. Hou, Supramolecular self-assembly of macroscopic tubes, Science 303 (2004) 65–67.
[7] C.H. Cai, L.Q. Wang, J.P. Lin, Self-assembly of polypeptide-based copolymers into diverse aggregates, Chem. Commun. 47 (2011) 11189–11203.
[8] A.O. Moughton, M.A. Hillmyer, T.P. Lodge, Multicompartment block polymer micelles, Macromolecules 45 (2012) 2–19.
[9] M. Marguet, C. Bonduelle, S. Lecommandoux, Multicompartmentalized polymeric systems: towards biomimetic cellular structure and function, Chem. Soc. Rev. 42 (2013) 512–529.
[10] W.J. Zhu, J.P. Lin, C.H. Cai, The effect of a thermo-responsive polypeptide-based copolymer on the mineralization of calcium carbonate, J. Mater. Chem. 22 (2012) 3939–3947.
[11] Y. Zhang, W.L. Gao, Z.Y. Liu, et al., Mineralization and osteoblast behavior of multilayered films on TiO_2 nanotube surfaces assembled by the layer-by-layer technique, Chin. Chem. Lett. 27 (2016) 1091–1096.
[12] A. Dag, J.C. Zhao, M.H. Stenzel, Origami with ABC triblock terpolymers based on glycopolymers: creation of virus-like morphologies, ACS Macro Lett. 4 (2015) 579–583.
[13] F. Boato, R.M. Thomas, A. Ghasparian, et al., Synthetic virus-like particles from self-assembling coiled-coil lipopeptides and their use in antigen display to the immune system, Angew. Chem. Int. Ed. 46 (2007) 9015–9018.
[14] A. Klug, The tobacco mosaic virus particle: structure and assembly: Philos, Trans. R. Soc. Lond. B Biol. Sci. 354 (1999) 531–535.
[15] R.L. Garcea, L. Gissmann, Virus-like particles as vaccines and vessels for the delivery of small molecules, Curr. Opin. Biotechnol. 15 (2004) 513–517.
[16] X.B. Xiong, H. Uludağ, A. Lavasanifar, Virus-mimetic polymeric micelles for targeted siRNA delivery, Biomaterials 31 (2010) 5886–5893.
[17] K.K. Upadhyay, J.F. Le Meins, A. Misra, et al., Biomimetic doxorubicin loaded polymersomes from hyaluronan-*block*-poly(γ-benzyl glutamate) copolymers, Biomacromolecules 10 (2009) 2802–2808.
[18] C. Tamerler, M. Sarikaya, Genetically designed peptide-based molecular materials, ACS Nano 3 (2009) 1606–1615.
[19] J. Huang, C. Bonduelle, J. Thévenot, S. Lecommandoux, A. Heise, Biologically active polymersomes from amphiphilic glycopeptides, J. Am. Chem. Soc. 134 (2012) 119–122.
[20] Y.L. Li, T. Jiang, S.L. Lin, et al., Hierarchical nanostructures self-assembled from a mixture system containing rod-coil block copolymers and rigid homopolymers, Sci. Rep. 5 (2015) 10137.
[21] C.H. Cai, J.P. Lin, X.Y. Zhu, et al., Superhelices with designed helical structures and temperature-stimulated chirality transitions, Macromolecules 49 (2016) 15–22.
[22] C.H. Cai, Y.L. Li, J.P. Lin, et al., Simulation-assisted self-assembly of multicomponent polymers into hierarchical assemblies with varied morphologies, Angew. Chem. Int. Ed. 52 (2013) 7732–7736.
[23] X.Y. Zhu, Z. Guan, J.P. Lin, C.H. Cai, Strip-pattern-spheres self-assembled from polypeptide-based polymer mixtures: structure and defect features, Sci. Rep. 6 (2016) 29796.
[24] B. Tian, X.G. Tao, T.Y. Ren, et al., Polypeptide-based vesicles: formation, properties and application for drug delivery, J. Mater. Chem. 22 (2012) 17404–17414.
[25] L.X. Zhao, N.N. Li, K.M. Wang, et al., A review of polypeptide-based polymersomes, Biomaterials 35 (2014) 1284–1301.
[26] L.L. Chen, T. Chen, W.X. Fang, et al., Synthesis and pH-responsive schizophrenic aggregation of a linear-dendron-like polyampholyte based on oppositely charged polypeptides, Biomacromolecules 14 (2013) 4320–4330.
[27] J.P. Lin, J.Q. Zhu, T. Chen, et al., Drug releasing behavior of hybrid micelles containing polypeptide triblock copolymer, Biomaterials 30 (2009) 108–117.

[28] Z. Zhang, Q. Lv, X.Y. Gao, et al., pH-Responsive poly(ethylene glycol)/poly(L-lactide) supramolecular micelles based on host-guest interaction, ACS Appl. Mater. Interfaces 7 (2015) 8404–8411.
[29] X.W. Guan, Y.H. Li, Z.X. Jiao, et al., Codelivery of antitumor drug and gene by a pH-sensitive charge-conversion system, ACS Appl. Mater. Interfaces 7 (2015) 3207–3215.
[30] W. Agut, A. BrÛlet, C. Schatz, D. Taton, S. Lecommandoux, pH and temperature responsive polymeric micelles and polymersomes by self-assembly of poly[2-(dimethylamino)ethyl methacrylate]-*b*-poly(glutamic acid) double hydrophilic block copolymers, Langmuir 26 (2010) 10546–10554.
[31] A. Carlsen, S. Lecommandoux, Self-assembly of polypeptide-based block copolymer amphiphiles, Curr. Opin. Colloid Interface Sci. 14 (2009) 329–339.
[32] M.R. Talingting, P. Munk, S.E. Webber, Z. Tuzar, Onion-type micelles from polystyrene-*block*-poly(2-vinylpyridine) and poly(2-vinylpyridine)-*block*-poly (ethylene oxide), Macromolecules 32 (1999) 1593–1601.
[33] W.Q. Zhang, L.Q. Shi, Z.J. Miao, K. Wu, Y.L. An, Core–shell–corona micellar complexes between poly(ethylene glycol)-block-poly(4-vinyl pyridine) and polystyrene-block-poly(acrylic acid), Macromol. Chem. Phys 206 (2005) 2354–2361.
[34] Z.K. Zhang, R.J. Ma, L.Q. Shi, Cooperative macromolecular self-assembly toward polymeric assemblies with multiple and bioactive functions, Acc. Chem. Res. 47 (2014) 1426–1437.
[35] X.W. Jiang, Y. Wang, W.Q. Zhang, P.W. Zheng, L.Q. Shi, Raspberry-like aggregates containing secondary nanospheres of polystyrene-*block*-poly(4-vinylpyridine) micelles, Macromol. Rapid. Commun. 27 (2006) 1833–1837.
[36] J.F. Lutz, S. Geffroy, H. von Berlepsch, et al., Investigation of a dual set of driving forces (hydrophobic + electrostatic) for the two-step fabrication of defined block copolymer micelles, Soft Matter 3 (2007) 694–698.
[37] D.G. He, X.X. He, K.M. Wang, Y.X. Zhao, A facile route for shape-selective synthesis of silica nanostructures using poly-L-lysine as template, Chin. Chem. Lett. 24 (2013) 99–102.
[38] N.C. Wickremasinghe, V.A. Kumar, J.D. Hartgerink, Two-step self-assembly of liposome-multidomain peptide nanofiber hydrogel for time-controlled release, Biomacromolecules 15 (2014) 3587–3595.
[39] K. Matyjaszewski, J.H. Xia, Atom transfer radical polymerization, Chem. Rev. 101 (2001) 2921–2990.
[40] K.A. Davis, K. Matyjaszewski, Atom transfer radical polymerization of *tert*-butyl acrylate and preparation of block copolymers, Macromolecules 33 (2000) 4039–4047.
[41] Z.L. Zhuang, X.M. Zhu, C.H. Cai, J.P. Lin, L.Q. Wang, Self-assembly of a mixture system containing polypeptide graft and block copolymers: experimental studies and self-consistent field theory simulations, J. Phys. Chem. B 116 (2012) 10125–10134.
[42] Y.S. Yu, L.F. Zhang, A. Eisenberg, Morphogenic effect of solvent on crew-cut aggregates of apmphiphilic diblock copolymers, Macromolecules 31 (1998) 1144–1154.
[43] Y.Y. Wang, S.L. Lin, M.H. Zang, et al., Self-assembly and photo-responsive behavior of novel ABC_2-type block copolymers containing azobenzene moieties, Soft Matter 8 (2012) 3131–3138.
[44] Z.L. Zhuang, C.H. Cai, T. Jiang, J.P. Lin, C.Y. Yang, Self-assembly behavior of rod-coil-rod polypeptide block copolymers, Polymer 55 (2014) 602–610.
[45] L.F. Zhang, A. Eisenberg, Formation of crew-cut aggregates of various morphologies from amphiphilic block copolymers in solution, Polym. Adv. Technol. 9 (1998) 677–699.
[46] C. Harrison, D.H. Adamson, Z.D. Cheng, et al., Mechanisms of ordering in striped patterns, Science 290 (2000) 1558–1560.
[47] M. Pinna, X.H. Guo, A.V. Zvelindovsky, Block copolymer nanoshells, Polymer 49 (2008) 2797–2800.
[48] A. Horvat, G.J.A. Sevink, A.V. Zvelindovsky, A. Krekhov, L. Tsarkova, Specific features of defect structure and dynamics in the cylinder phase of block copolymers, ACS Nano 2 (2008) 1143–1152.
[49] L.S. Zhang, L.Q. Wang, J.P. Lin, Defect structures and ordering behaviours of diblock copolymers self-assembling on spherical substrates, Soft Matter 10 (2014) 6713–6721.
[50] H. Hopf, Vektorfelder in*n*-dimensionalen Mannigfaltigkeiten, Math. Ann. 96 (1927) 225–249.